

Miscibility and thermal properties of blends of melamine–formaldehyde resin with low density polyethylene

W. Brostow*^{1,2} and T. Datashvili¹

Blends were prepared using a Brabender preparation station and compression moulding. Characterisation included differential scanning calorimetry (DSC), thermogravimetric analysis (TGA), Fourier transform infrared spectroscopy (FTIR), environmental scanning electron microscopy (ESEM) and atomic force microscopy (AFM). Thermal analysis, AFM and ESEM support the occurrence of a partial compatibilisation. In particular, the DSC results showed that the melting peaks intermediate between those of pure components.

Keywords: Melamine–formaldehyde resin, LDPE, Blend, Miscibility, FTIR, DSC

Introduction

Demands are growing for improvement of mechanical and/or tribological properties of polymer based materials (PBMs).^{1,2} Polymer blends and/or polymers with fibres or fillers can provide properties unattainable in pure components.^{3–13} Melamine–formaldehyde resins (MFR) have been synthesised and blended with a low density polyethylene (LDPE) to improve LDPE properties. A variety of techniques have been used to determine the miscibility behaviour and thermal properties of the blends as potential design materials for the plastics industry.

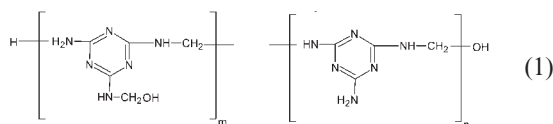
Experimental

Materials

Low density polyethylene was from Aldrich Chemicals Co. Melamine C₃H₆N₆ (2,4,6–triamino–1,3,5–triazine), formaldehyde CH₂O and sodium hydroxide NaOH were from Fluka and Sigma Chemicals Co. respectively.

Synthesis of melamine–formaldehyde resin

Melamine–formaldehyde resin was synthesised from melamine by polycondensation reaction with formaldehyde in a basic medium. The molar ratio of melamine–formaldehyde was from 1 to 3. The pH value of formaldehyde (37.0 wt-% in water) was adjusted to 7.5–8.0 by adding 10 wt-%NaOH (aq.). The resulting solution was placed in a beaker and thoroughly mixed with 20 g melamine; the components were then stirred for 40 min at 120°C. The resulting structure is



Final product was subjected to evaporation at 70°C at 13–16 kPa, followed by drying at 80°C for 24 h.

Blending and sample preparation

Dried PE and MFR were melt mixed in a CW Brabender D–52 Preparation Station at 80 rev min⁻¹ and 160°C. The resulting blends were pelletised and dried. The blends contained in turn were 1, 5, 10, 20 and 25 wt-%MFR. Subsequently, the blends were dried for 8 h at 100°C before being compressed in a Carver compression moulding machine at 160°C at the pressure of 20.7 × 10³ kPa.

Differential scanning calorimetry

Differential scanning calorimetry (DSC) measurements were performed on a Perkin Elmer DSC–7 instrument.^{14,15} The temperature ranged from –100 to 300°C and the heating rate was 10 K min⁻¹ under N₂. A sealed liquid type Al capsule pan was used. Melting temperatures *T*_m were evaluated on the basis of thermo grams.

Thermogravimetric analysis

All the blend samples were dried in an oven at 100°C for 1 h before being analysed by thermogravimetric analysis (TGA) in N₂ atmosphere at the heating rate of 10 K min⁻¹. Isothermal thermogravimetry was used to determine a temperature profile on a Perkin Elmer TG–7 instrument. Several milligrams of each dried sample were placed on a balance located in the furnace that was heated from +50 to 600°C.

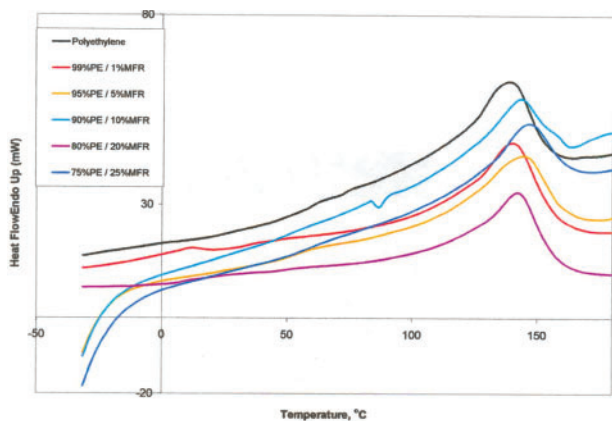
Fourier transform infrared spectroscopy

The spectra were recorded on a Nexus 470 Fourier transform infrared spectroscopy (FTIR) ESP Series

¹Laboratory of Advanced Polymers & Optimized Materials (LAPOM), Department of Materials Science and Engineering, University of North Texas, Denton, TX 76203 5310, USA

²College of Mechanics and Robotics, AGH University of Science and Technology, Adama Mickiewicza 30, 30 059 Cracow, Poland

*Corresponding author, email brostow@unt.edu



1 Differential scanning calorimetry thermograms of LDPE and LDPE+MFR blends

spectrometer at the resolution of 4 cm⁻¹ in the mid infrared range from 4000 to 800 cm⁻¹. To enhance the signal to noise ratio, each of the reference and sample spectra presented constitutes the average of 68 recorded scans. All blend systems were used in the solid state. Following an established procedure,^{16,17} the indexes were calculated as

$$\text{secondary amine index} = \frac{I_{1550}}{I_{3345}} \times 100 \quad (2)$$

Environmental scanning electron microscopy

Micrographs of PE, MFR and all blends were taken using a FEI Quanta environmental scanning electron microscopy (ESEM). Some samples were fractured in liquid N₂ mounted on a copper stub and coated with a thin layer of gold to avoid electrostatic charging.

Atomic force microscopy

Nanoscope III atomic force microscopy (AFM) from Veeco Digital Instruments was used to study the roughness and morphology of the blends. Standard silicon nitride contact mode probes were used.

Table 1 Melting temperatures of LDPE+MFR blends

Composition	Melting temperatures, °C
LDPE	139.4
99% LDPE	139.7
95% LDPE	140.8
90% LDPE	141.8
80% LDPE	143.7
75% LDPE	145.2

Thermal properties

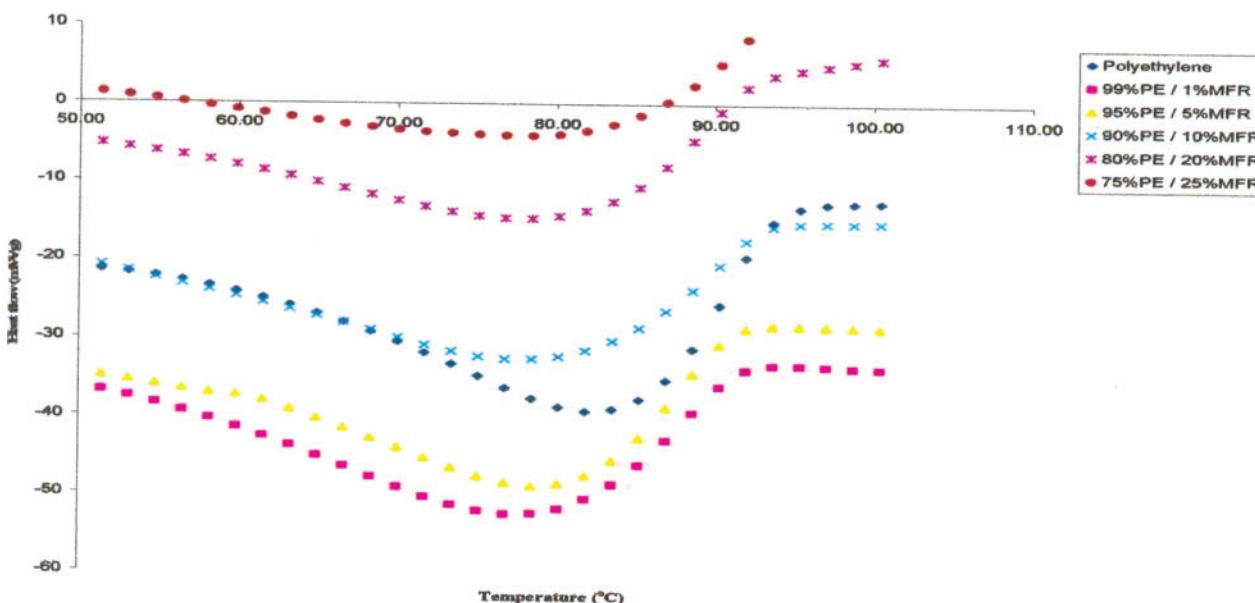
Thermal characterisation of polymer blends is a well known method for the determination of their miscibility.¹⁴ Differential scanning calorimetry curves for several compositions are shown in Fig. 1. All the blends show melting peaks in the 140–150°C regions, intermediate between melting temperatures *T_m* of two pure components (Table 1).

All the blends studied displayed exotherms in the temperature range of 80–100°C, between the crystallisation temperatures *T_c* of PE and MFR. The exotherms are shown in Fig. 2. Upon the addition of MF resin, the *T_c* values are shifted to lower values than that for pure LDPE. The authors concluded that their blends are miscible in the amorphous state.

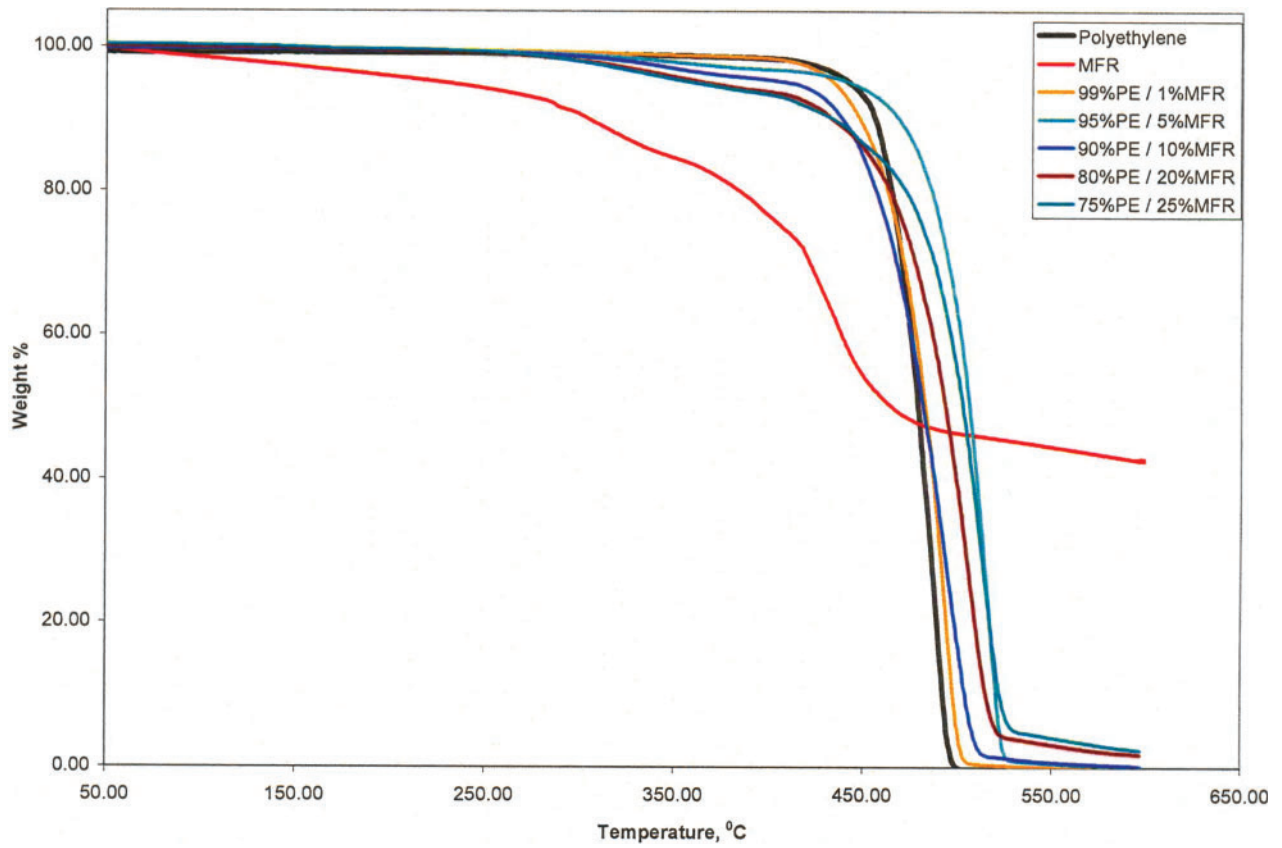
The TGA curves of the MFR, LDPE and all blends are shown in Fig. 3 and clearly show better thermal stability of all blends as compared to the pure components. Thus, both LDPE and MFR gain by the addition of the second component. All the cured blends exhibit thermal stability up to 300°C. The TGA derivative curves in Fig. 4 show that the weight loss increases noticeably above 500°C.

Fourier transform infrared spectroscopy analysis

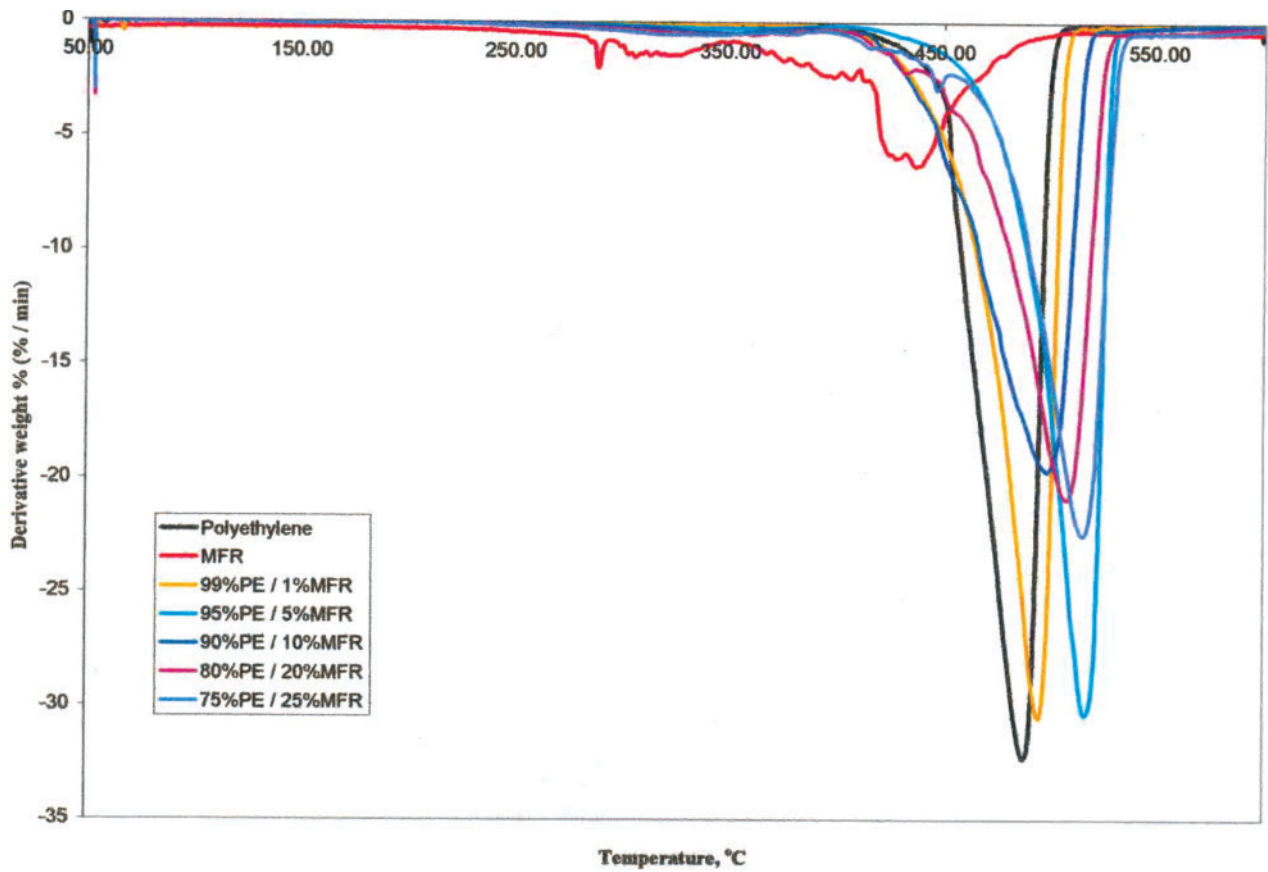
Fourier transform infrared spectroscopy analysis is known as a suitable method to determine the presence of specific interactions between various groups in



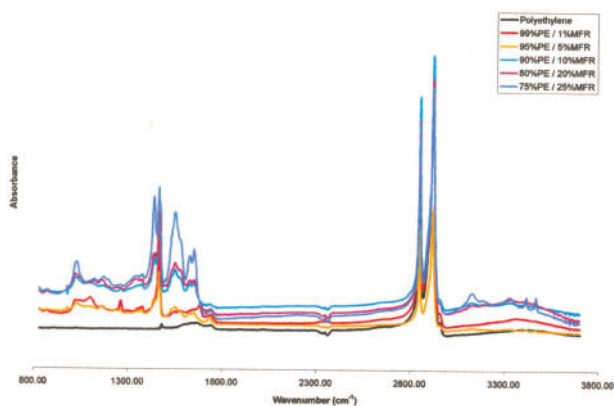
2 Differential scanning calorimetry thermograms of LDPE and LDPE/MFR blends



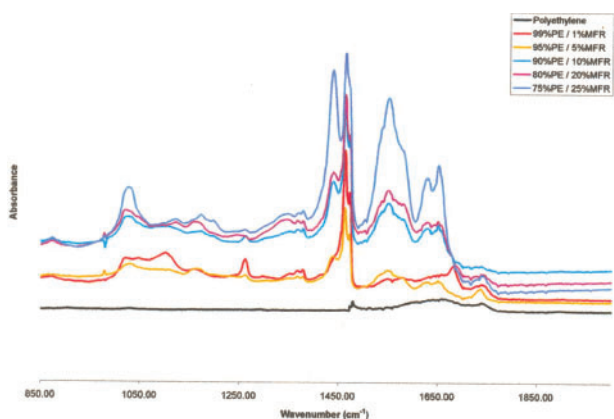
3 Thermogravimetric analysis scans of LDPE+MFR compositions



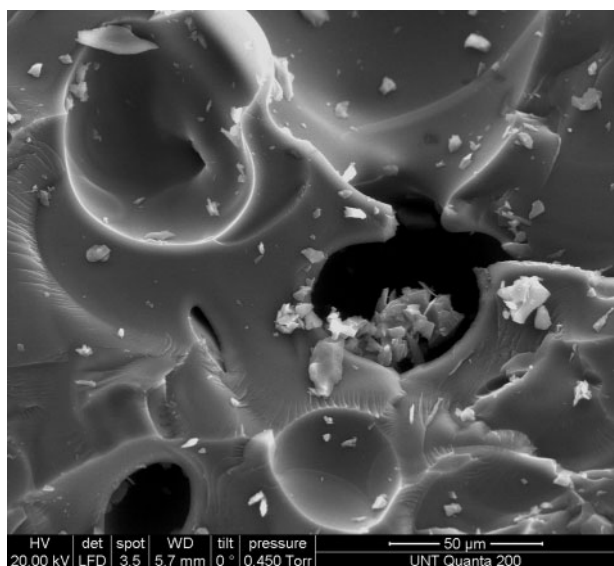
4 Derivatives of PE, MFR and PE+MFR blends from TGA scans



5 Fourier transform infrared spectroscopy spectra for blends and pure LDPE



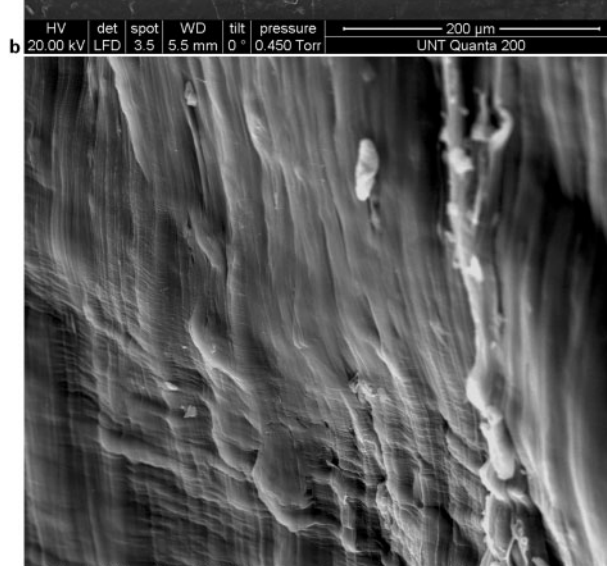
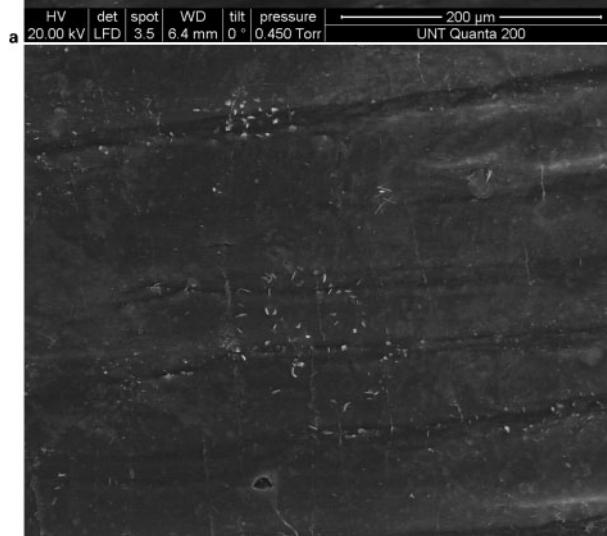
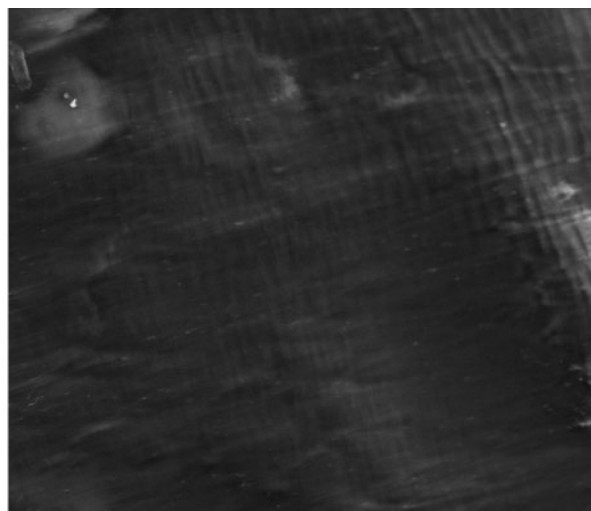
6 Fourier transform infrared spectroscopy spectra for 850–2000 cm^{-1} region of blends and LDPE



7 Images (ESEM) of MFR

polymer blends. It is sensitive to both inter- and intramolecular interactions.¹⁸ Figure 5 shows the FTIR spectra for all blends and LDPE.

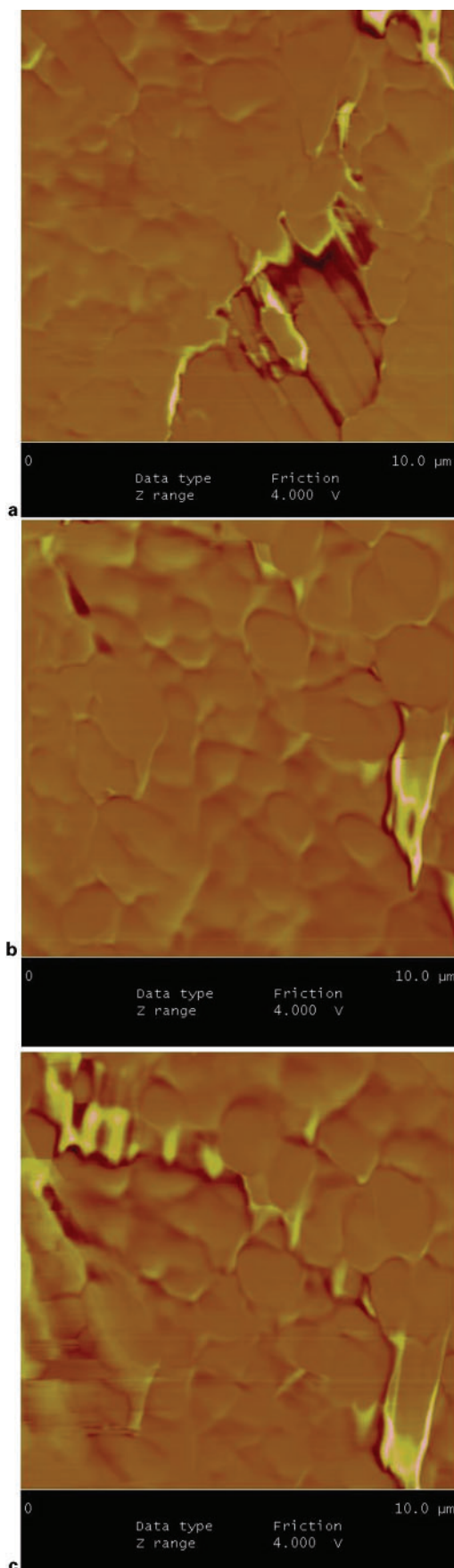
The blends containing 1 and 5 wt-%MFR exhibited no stretching vibration of –OH in the 3000–3600 cm^{-1} range. The vibration seemed to appear at higher concentrations of MFR as small peaks. These peaks are characteristic for the –OH fragments of the MFR. A



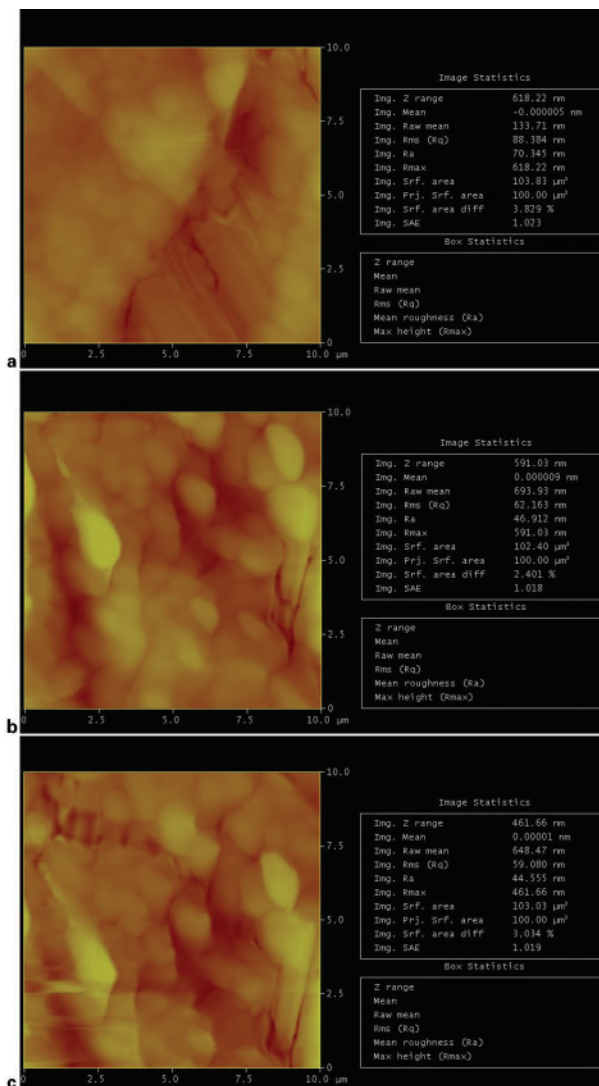
8 Scanning electron micrographs of cryogenically fractured surfaces of blends containing a 10, b 20 and c 25 wt-%MFR

small portion of these –OH groups appeared along with increasing concentration of MFR though not evidence for hydrogen bonds between the PE and MFR.

High peaks in the region 2800–3000 cm^{-1} are associated with the methylene (–CH₂–) and dimethylene



9 Images (AFM) of blends containing a 10, b 20 and c 25 wt-%MFR



10 Roughness analysis of blends containing a 10, b 20 and c 25 wt-%MFR

(–CH₂–CH₂–) stretching of the polyethylene. Also note the N–H stretching peak in the 3000–3600 cm⁻¹ range. The functional group changes in the blends, as Fig. 6 shows the expanded scale FTIR spectra in the 850–2000 cm⁻¹ region at room temperature (24°C) for several blend compositions. The formation of peaks is observed in Fig. 6 in the 800–1700 cm⁻¹ region. These signals are characteristic for the MF resin and are larger at higher MFR concentrations.

Other characteristic peaks for the MF resin are the absorption bands in the 1546–1558 cm⁻¹, 1635–1648 cm⁻¹ and 1006–1022 cm⁻¹ range. The 1546–1558 cm⁻¹ range corresponded to the secondary aromatic amine, while the 1635–1648 cm⁻¹ range corresponded to the NH₂ vibration. The peaks increased in size, as expected, with increasing MF resin contents.

Blends morphology

The roughness and morphology of the LDPE + MFR blends are seen in the AFM and ESEM images. Figure 7 shows an ESEM micrograph of the MF resin, a typical case of brittle fracture. The fracture paths are mostly straight and constitute failure bands.

Figure 8 shows SEM results for the blends.

Images (ESEM and AFM) obtained from the blends show similar morphologies; LDPE and MFR are partially miscible and the extent of phase separation is low, as shown in Figs. 9 and 10.

From the AFM measurements performed for the blends, the microscopic roughness (root mean square value) was determined to be 59.1–88.4 nm over the whole composition range, for an area of $10 \times 10 \mu\text{m}$.

Acknowledgements

Partial financial support has been provided by the Robert A. Welch Foundation, Houston, TX, (grant no. B–1203), and also initially by the Georgian Research Development Foundation (GRDF), Tbilisi, via a fellowship to an author (T. Datashvili).

References

1. W. Brostow: in 'Performance of plastics', (ed. W. Brostow), Chap. 5; 2000, Munich, Cincinnati, Hanser Gardner.
2. W. Brostow, J. L. Deborde, M. Jaklewicz and P. Olszynski: *J. Mater. Ed.*, 2003, **24**, 119.
3. M. Aubin, Y. Bedard, M. F. Morrissette and R. E. Prud'homme: *J. Polym. Sci. Phys.*, 1983, **21**, 233.
4. R. Fayt, R. Jérôme and P. Teyssié: *J. Polym. Sci. Phys.*, 1989, **27**, 775.
5. W. Brostow, B. Bujard, P. E. Cassidy, H. E. Hagg and P. E. Montemartini: *Mater. Res. Innov.*, 2002, **6**, 7.
6. M. Garcia, J. I. Eguiazabal and J. Nazabal: *J. Appl. Polym. Sci.*, 2001, **81**, 121.
7. W. Brostow, P. E. Cassidy, H. E. Hagg, M. Jaklewicz and P. E. Montemartini: *Polymer*, 2002, **42**, 7971.
8. B. Bilyeu, W. Brostow and K. P. Menard: *Polym. Compos.*, 2002, **23**, 1111.
9. L. Sharma and T. Kimura: *Polym. Adv. Technol.*, 2003, **14**, 373.
10. R. Palkovits, H. Althues, A. Ruplecker, B. Tesche, A. Dreier, U. Holle, G. Fink, C. H. Cheng, D. F. Shantz and S. Kaskel: *Langmuir*, 2005, **21**, 6048.
11. W. Brostow, M. Keselman, I. Mironi-Harpaz, M. Narkis and R. Peirce: *Polymer*, 2005, **46**, 5058.
12. R. Perez, E. Rojo, M. Fernandez, V. Leal, P. Lafuente and A. Santamaria: *Polymer*, 2005, **46**, 8045.
13. S. Jose, S. Thomas, E. Lievana and J. Karger-Kocsis: *J. Appl. Polym. Sci.*, 2005, **95**, 1376.
14. K. P. Menard: in 'Performance of plastics', (ed. W. Brostow), Chap. 8; 2000, Munich, Cincinnati, Hanser Gardner.
15. B. Bilyeu, W. Brostow and K. P. Menard: *J. Mater. Ed.*, 2000, **22**, 107.
16. S. Kim and H. J. Kim: *Adhes. Sci. Technol.*, 2006, **20**, 209.
17. S. Garnier, A. Pizzi, O. C. Vorster and L. Halasz: *J. Appl. Polym. Sci.*, 2002, **86**, 852.
18. D. Tuncer and H. Salim: *Building Environ.*, 2004, **39**, 1199.